Experimental Characterization of the Impedance of Balanced UHF RFID Tag Antennas

C. K. Stoumpos[1], D. E. Anagnostou[2], and M. T. Chryssomallis[1]
[1]Department of Electrical and Computer Engineering, Democritus University of Thrace, Xanthi, 67100, Greece
Corresponding author: danagn@ieee.org
[2] Institute of Sensors, Signals and Systems, Heriot Watt University, Edinburgh, EH14 4AS, United Kingdom

Received 11 May, 2017

ABSTRACT–*An experimental procedure for the accurate characterization of the impedance of balanced tag antennas for RFID applications is re introduced. The balanced devices that are characterized are modeledas two-port networks and their impedance is derived from network parameters, through a rarely used equation that is preferred because it accounts for the losses of non-reciprocal structures such as imperfect test fixtures or baluns. The measurements are conducted using a test fixture for the proper excitation of the balanced devices, and its effects are removed by shifting the measurement plane to the plane of the device under test. The accuracy of the proposed method is demonstrated through the measurement of the impedance of a balanced dipole antenna, and is complemented by the measurement of the RFID ASIC chip. The experimental characterization of the impedance of an RFID tag antenna constitutes a secure way to achieve conjugate matching between the two devices (i.e. the antenna and the RFID chip), and finally enhance the reading range of the RFID tags. Also, since RFID tags are designed to be placed directly on different surfaces, the proposed procedure is further evaluated by mounting the antenna onto two more surfaces.*

Key words: *Balanced antenna, chip, impedance, integrated components, RFIC, RFID, paper substrate, passive structures, tag, wire antennas.*

1. INTRODUCTION

RF IDENTIFICATION (RFID) is a rapidly developing technology with roots back to 1948 that achieves wireless and automatic data collection through a reader device and an RFID tag, using RF signals [1, 2]. The tag is typically a metallic coplanar antenna printed on a substrate, and is commonly a dipole on whose terminals an integrated circuit (IC) or chip is mounted. The RFID tag receives, modulates and backscatters the RF signal that is transmitted from the reader. RFID tag antennas must be conjugate matched to the complex impedance of the RFID chip [3] for their performance to be maximized. They also differ from traditional antenna systems, as an external matching network is not feasible due to cost and size limitations.

In most RFID applications, the tag is affixed on different objects with surfaces of varying size, material composition and electrical properties, which alter the impedance of the tag antenna, leading to mismatch and therefore deterioration of the reading range [4]. Consequently, the tag designers design usually a tag antenna for a specific application, taking into account the arisen limitations. The experimental characterization of the antenna impedance and IC of a tag validates and assures that a sufficient conjugate matching is achieved. The strong dependence of the conjugate match of an RFID tag with the reading range is illustrated by Friis' free-space formula and is presented in [5,6]:

$$r_{\max} = \frac{\lambda}{4\pi}\sqrt{\frac{P_t G_t G_r \left(1-|s|^2\right)}{P_{th}}} \qquad (1\text{-}1)$$

where P_t is the power transmitted by the RFID reader, G_t is the gain of the transmitting antenna (P_tG_t is the EIRP, equivalent isotropic radiated power), G_r is the gain of the receiving tag antenna, and P_{th} is the minimum threshold power necessary to power up the chip. Typically, the power reflection coefficient is that, which primarily determines the resonance of the tag and is calculated as:

$$|s|^2 = \left|\frac{Z_{Ant} - Z_{Chip}^*}{Z_{Ant} - Z_{Chip}}\right|^2 \qquad (1\text{-}2)$$

where Z_{Ant} and Z_{Chip} are the complex impedances of the antenna and chip of the tag, respectively and * means complex conjugate.

In this work, the measurements of three balanced devices are presented. According to the impedance model of balanced devices and the relative measurement procedure, the input impedance of a linear wire dipole antenna is extracted, in order to validate the proposed methodology. The input impedance of an RFID tag antenna and of its IC are also measured in laboratory environment through a vector network analyzer (VNA) and extracted by the S-parameters. Last but not least, the impedance of the antenna of the RFID tag is measured on three different surfaces and the input impedance is calculated. The method, its validation using the dipole antenna and the additional presented results comprise a useful set of data to an RFID design and test engineer. The structure of this paper is organized as follows. Section 2 describes the main principle that characterizes balance devices and how their impedance is extracted. Section 3 presents the experimental procedure chosen, Section 4 presents the experimental results and Section 5 presents the conclusions.

The structure of this paper is organized as follows. Section II describes the main principle that characterizes balance devices and how their impedance is extracted. Section III presents the experimental procedure chosen, Section IV presents the experimental results and Section V presents the conclusions.

2. IMPEDANCE CHARACTERIZATION METHODOLOGY

Since RFID tag antennas are – in their majority – balanced devices, but most instruments are terminated to unbalanced ports (e.g. the coaxial test ports of a common VNA), during an antenna measurement the problem of common-mode

excitation arises and leads to unequal feeding currents to the arms of balanced antennas. The two traditional methods that try to eliminate the problem of inequality of feeding current, and thus to extract quite accurate results for the input impedance of balanced antennas, are (i) the use of a balun [7], which forces an equal current flow towards the two antenna arms, and (ii) the imaging method [8, 9], by mounting half a radiator on a ground plane, which provides a mirror image. The first method relies on how ideal the balun is and the second method relies on the size of the ground plane and can be used only with symmetrical antennas.

Based on [10], the input impedance of a symmetrical balanced antenna can be characterized through *S*-parameters derived through a VNA. The VNA is terminated to coaxial ports, so the introduction of a test fixture with coaxial to microstrip transition and differential feeding is needed. Fig. 1 shows the test fixture used for the measurements of balanced loads. The common ground (therefore, differential excitation too) is achieved by soldering the outer semi-rigid conductors of the test fixture together, whereas the tips on the edge are connected to the device under test (DUT). The effects of the test cables must be removed, and for this reason the de-embedding technique is used to shift mathematically the measurement plane to the device plane. Fig. 2 shows the configuration of the DUT and the currents and voltages for the balanced antenna model.

The antennas are then modeled as a two-port network with common ground between their radiators, and after the circuit analysis and parameter transformations [11], the equation, which yields the input impedance of a balanced load from the S-parameters, is derived:

$$Z_d = \frac{2Z_0\left(1-S_{11}S_{22}+S_{12}S_{21}-S_{12}-S_{21}\right)}{\left(1-S_{11}\right)\left(1-S_{22}\right)-S_{21}S_{12}} \qquad (2\text{-}1)$$

Equation (2-1) differs from the rather common and simplified version, equation (2-2), which is used exclusively for symmetrical balanced antennas and which indicates that the devices under test are balanced. The simplified equation assumes that $S_{11} = S_{22}$ and $S_{12} = S_{21}$, then:

$$Z_d = \frac{2Z_0\left(1-S_{11}^2+S_{21}^2-2S_{12}\right)}{\left(1-S_{11}\right)^2-S_{21}^2} \qquad (2\text{-}2)$$

It is notably significant that the measurements extracted from the simplified equation (2-2) yield incorrect results, unless the fixture halves have precisely identical lengths and therefore there is no phase difference between them. Thus, for the results presented in this paper, equation (2-1) has been used.

Before the mathematical process of de-embedding is developed, the test fixture, after its characterization, and the DUT are represented as three separate two-port networks (Fig. 2). This is a convenient form because the *T*-parameters can then be exploited [12], and then their respective *T*-matrices (T_A, T_{DUT} and T_B) can be easily multiplied:

$$[T_{MEASURED}] = [T_A][T_{DUT}][T_B] \qquad (2\text{-}3)$$

This matrix operation will represent the *T*-parameters of the test fixture and DUT when measured by the VNA at the measurement plane. The final goal is the two sides of the fixture, T_A and T_B, to be de-embedded and information about the DUT or T_{DUT} to be gathered. The de-embedding procedure can be illustrated by the following equation of matrices:

$$[T_{DUT}] = [T_A]^{-1}[T_A][T_{DUT}][T_B][T_B]^{-1} \qquad (2\text{-}4)$$

In this way, the matrix inversion of T-parameters is exploited and extended to the case of cascaded fixture and DUT matrices. Therefore, the T-parameters for the DUT can be extracted and after converting them back to S-parameters, the calculation of the input impedance for each DUT will be found using (2-1).

Figure 1 The test fixture used for the measurement of balanced devices.

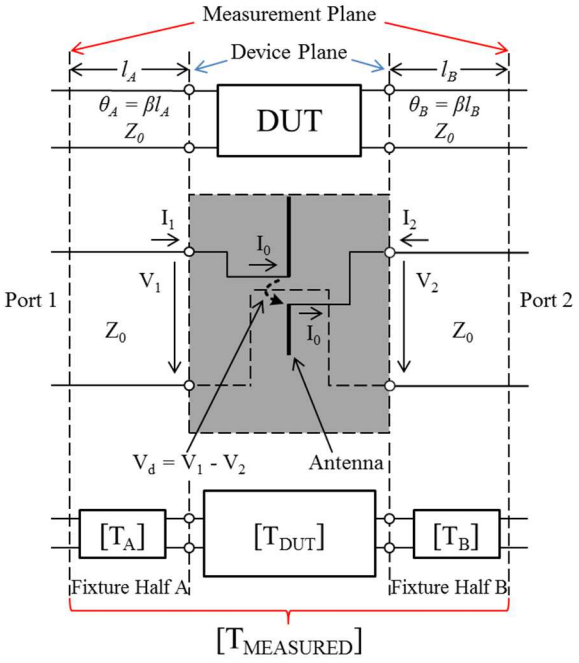

Figure 2 Configuration of the DUT with the two test fixture halves presenting the measurement and the device plane. The balanced antenna as a two-port network is also illustrated.

3. EXPERIMENTAL PROCEDURE

The measurements took place in laboratory environment were a VNA was used for the extraction of *S*-parameters of the DUT. The configuration of the measurement setup is shown in Fig. 3. The measurement plane is on the tips of the test fixture, whereas the VNA is also calibrated to the test fixture connector's plane so that its systemic errors could be corrected. After that, the de-embedding technique was used so that the effect of the test fixture could be eliminated and finally the shift of the measurement plane to the device plane could be achieved. The test fixture is constructed by two semi-rigid coaxial cables with a length of approximately 65 mm and an outer conductor diameter of 3 mm. The one end of the test fixture leads to two SMA (SubMiniature version A) connectors which are connected to the test cables of the VNA, whereas the other end is open with the small extensions of the inner conductors forming the tips where each DUT is soldered onto. The measurement can be conducted via the following steps:

1. The VNA is calibrated at the SMA connectors using the manufacturer's calibration standard kit.
2. Short-circuiting the test fixture (soldering the tips of the test fixture and outer conductors of the coaxial cables together) yields its parameters.
3. The parameters of the DUT free from the effects of the test fixture (or equivalently the shift of the measurement plane to the device plane), after being measured by the VNA, can be extracted using the de-embedding technique of equation (2-4).
4. The input impedance of the DUT can then be extracted using equation (2-1).

Figure 3 Measurement setup using Agilent HP8510C network analyzer.

4. MEASUREMENT RESULTS

Typical results are presented for a dipole antenna, an RFID ASIC (Application Specific Integrated Circuit) and an RFID tag antenna in three cases.

4.1. Dipole Antenna Validation

For validation purposes, a typical linear balanced dipole antenna was constructed and measured. Two pieces of copper wire 0.5 mm thick, were soldered onto the inner conductors of the semirigid cables of the test fixture, yielding the dipole configuration. The total length was 173.4 mm and was chosen as the half-wavelength that corresponds to the central frequency of 866 MHz, the European RFID tag band. The dipole was mounted onto a sheet of paper for mechanical stability. Fig. 4a shows the dipole antenna under test and the measurement configuration.

Fig. 4b shows the measured and simulated input impedance of the dipole antenna from 800 to 1000 MHz. The simulation was conducted with IE3D™ [13], which is based on the method of moments. The measured input impedance results were extracted using equation (2-1). The measurements compare well in form and value with the results computed by the simulation, as well as with the theoretical value of 73 + j42.5 Ω, further validating the method. The measurement results show only a difference in amplitude, particularly at the frequency range above 900 MHz for the imaginary part - an occurrence due to the small gap between the dipole arms and the proximity of the feeding cables.

4.2. RFID ASIC Measurement

The second set of measurements included the ASIC of the RFID tag antenna. For manufacturing considerations, RFID chip manufacturers supply the customers with RFID straps rather than chips [14]. The ASIC is mounted with conductive glue on the terminal pads of the strap and by this structure the tag-antenna is excited (Fig. 5a). The Alien Higgs 3 IC was extracted from the ALN 9662 Short Inlay RFID tag, and its terminal pads and the RFID strap under test were soldered onto the test fixture so as the measurements could be conducted (Fig. 5b).

According to the manufacturer's datasheet [15], the Alien Higgs 3 IC presents an equivalent input impedance of R_{chip} = 1500 Ω and C_{chip} = 0.85 pF in parallel connection, for an input power of -14 dBm over the range of 860-960 MHz. Therefore, the series input impedance of the chip is Z_{chip} = 30.53 – j211.81 Ω for the abovementioned specifications.

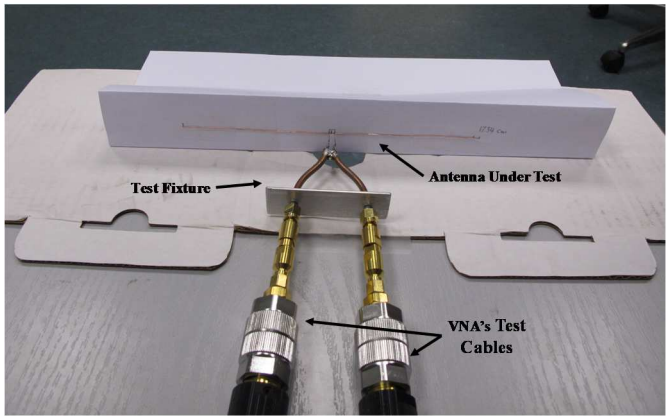

(a)

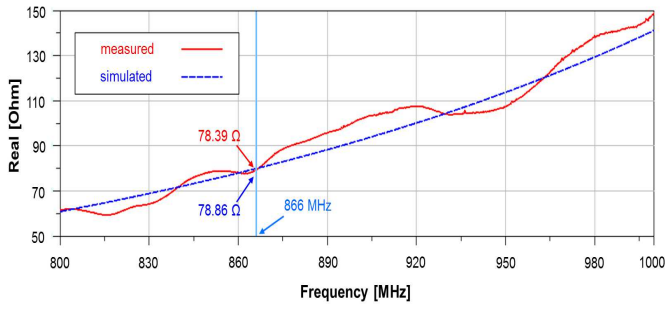

(b)

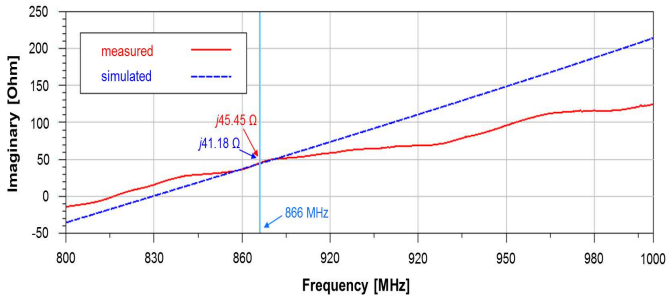

(c)

Figure 4 Configuration and measured (red solid line) and simulated (blue dashed line) impedance of the dipole antenna. (a) Measurement of Dipole antenna. (b) Real part. (c) Imaginary part.

The goal was for the input impedance of the RFID strap to be measured over a wide range of input power, where the results could be compared to those of the manufacturer and moreover the threshold power could be detected. Thus, the RF output power of the network analyzer was swept from −18 to +3 dBm and the measurement data were recorded. However, the RF output power of the network analyzer is not equal to the actual absorbed power of an RFID strap, due to mismatch between the impedance of the RFID strap and the 50 Ω impedance of the test fixture and the coaxial cable of the network analyzer [16]. Therefore, the sweeping RF output power P_{RF} was corrected with the power reflection coefficient [17]. The absorbed power P_{strap} can be compensated by:

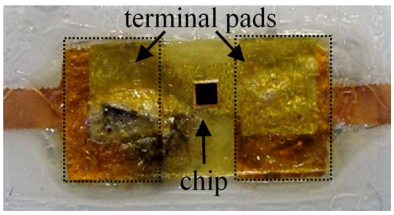

(a)

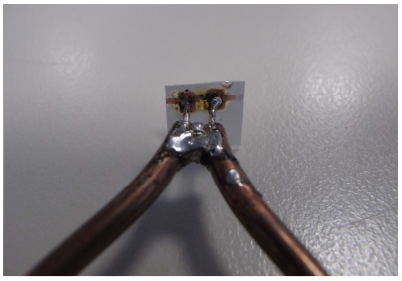

(b)

Figure 5 Photograph of the RFID strap Alien Higgs 3 IC (chip with its terminal pads). (a) Front view. (b) Soldered onto test fixture.

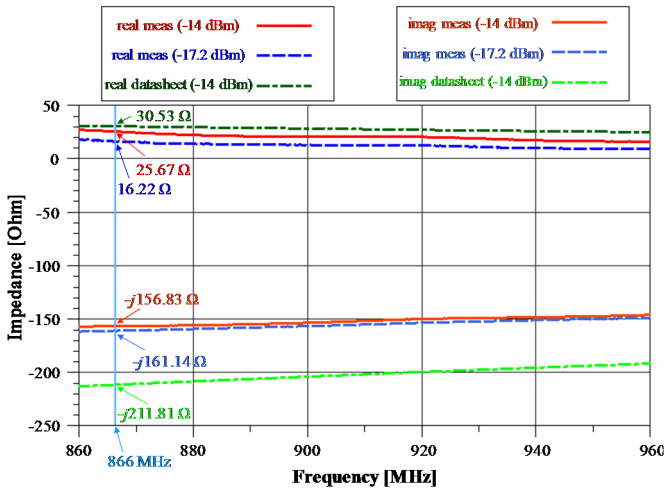

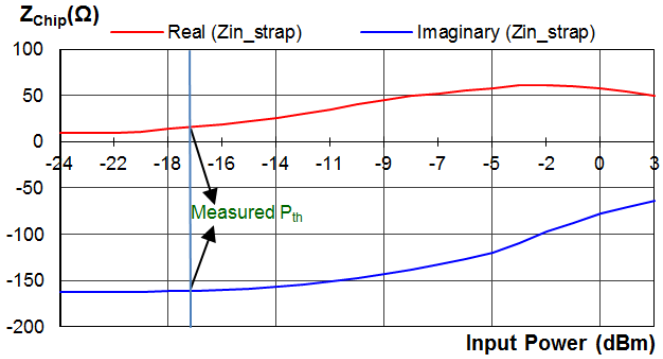

Figure 6 Measured chip impedance.
(a) Measured (at -14 dBm and -17.2 dBm) and simulated from manufacturer datasheet's equivalent circuit (at -14 dBm)
(b) Measured chip impedance versus absorbed power at 866 MHz, where the threshold power is defined.

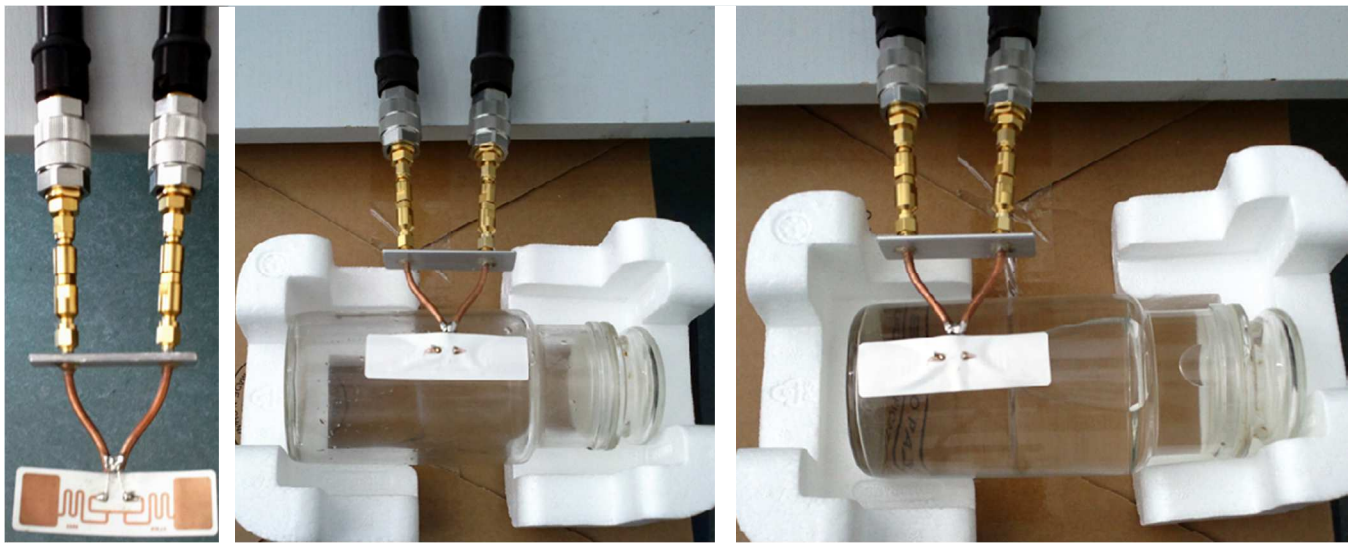

(a) (b) (c)

Figure 7 Measurement setup of the antenna of the RFID tag on three different material surfaces. (a) Air. (b) Empty glass object. (c) Filled with water glass object.

$$P_{strap} = P_{measured} + 10 \cdot \log\left(1 - \left|\Gamma\right|^2\right) \qquad (4\text{-}1)$$

and the power reflection coefficient is given by applying (1-1) for minimum reflected wave conditions:

$$\left|\Gamma\right|^2 = \left|\frac{Z_0 - Z_{Strap}}{Z_0 + Z_{Strap}}\right|^2 \qquad (4\text{-}2)$$

Now, P_{strap} is the actual absorbed power of the RFID strap and all measurement results can be postprocessed and corrected. Fig. 6a shows the measured RFID strap (the chip with terminal pads) impedance at -14 dBm and -17.2 dBm and the simulated impedance of the strap using the manufacturer's values at -14 dBm. It can be seen that the measurement compares well in form and value with the simulation results. The measured results show only a difference in amplitude for the imaginary part. The deviation was attributed to the fact that the measurement was conducted for the RFID strap, which includes a piece of the substrate of the tag, the conductive glue and the terminal pads where the chip is leaded at, whereas the manufacturer's values refer to the standalone chip. Fig. 6b illustrates the measured strap impedance versus the absorbed power from the VNA at 866 MHz. The threshold power (the activation power level) of the RFID strap was defined from the measurements (Fig. 7) at -17.2 dBm.

4.3. RFID Tag Antenna Measurement

For the third case, the antenna under test was the RFID ALN-9662 Short Inlay tag antenna by Alien Technology, which follows the ISO 18000-6C (Class 1, Gen2) standard over the frequency range of 860-960 MHz. Three sets of impedance measurements took place. The first included the tag antenna under test suspended in the air, the second placed onto an empty glass container and the third placed onto a glass container filled with water. Figure 7 presents the measurement setup for these three cases where the RFID tag antenna was measured. The particular RFID tag antenna is fabricated by printing aluminium onto a 38 μm thick PET (Polyethylene Terephthalate) substrate with ε_r = 3.8 and tanδ = 0.02. The manufacturer supplies the RFID tag antenna with conductive glue and a piece of paper, which was removed during the measurement.

Fig. 8 presents the measured impedance of the antenna of the RFID tag for the cases of air and empty glass. The small reduction in both the real and imaginary parts of the antenna impedance is due to its mounting onto the glass. Fig. 9 presents the measured impedance of the RFID tag antenna when mounted onto a glass filled with water, over the same frequency range. A high increase in both real and imaginary parts is observed, due to the presence of water into the glass.

Figure 9 presents the measured impedance of the antenna of the RFID tag for the cases of air and empty glass. The small reduction in both the real and imaginary parts of the antenna impedance is due to its mounting onto the glass. Figure 10 presents the measured impedance of the RFID tag antenna when mounted onto a glass filled with water, over the same frequency range. A high increase in both real and imaginary parts is observed, due to the presence of water into the glass.

Figure 10 illustrates the return loss of the RFID tag antenna for the three aforementioned cases, where the measured input impedance of the RFID ASIC was taken at the detected threshold power. The return loss was extracted using the following equation [18]:

$$RL = -20 \cdot \log\left|\frac{Z_{Tag} - Z_{Chip}^*}{Z_{Tag} + Z_{Chip}}\right| \qquad (4\text{-}3)$$

where Z_{tag} the input impedance of the antenna of the RFID tag measured onto each surface, and Z_{chip} the input impedance of the RFID chip measured at threshold power. It can be seen, that for the first two cases, the return loss of the RFID tag antenna is small enough, whereas for the third case it is degraded due to the presence of water into the glass onto which the tag is mounted.

5. CONCLUSION

An experimental methodology for the characterization of the impedance of the balanced RFID tag antennas has been implemented. By using a two-port measurement and the deembedding technique, the impedance of a balanced dipole was extracted directly from the *S*-parameters with the use of the appropriate equation. After validating the methodology with a dipole, two sets of measurements took place in lab environment. The measurement of the input impedance of an RFID strap for different levels of input power showed rather good results in reference to theoretical and expected values. The deviations from the manufacturer's datasheet values are considered as expected and are attributed to the fact that the measurements of the RFID ASIC were conducted on the terminal pads of the strap, which included conductive adhesive. Finally, the input impedance measurement of an RFID tag antenna onto three different material surfaces was conducted and the return loss was extracted for every case. The results, are evaluated largely as expected, as the input impedance of the tag antenna was measured and characterized close enough to the conjugate impedance of the RFID strap for the first two cases, whereas a large degradation was found for the third case measurement of the filled with water glass container. These results validate the importance of the work of antenna designers and justify the development of application-specific RFID tags when they are used with different objects. Moreover, the presented results and methodology can be a useful toolkit for the RFID design and test engineer, and of particular usefulness as a guide for accurate measurements using imperfect test fixtures.

ACKNOWLEDGMENTS

The authors want to thank Professor J. Sahalos for the provision of RFID tags and his valuable help and comments for this work.

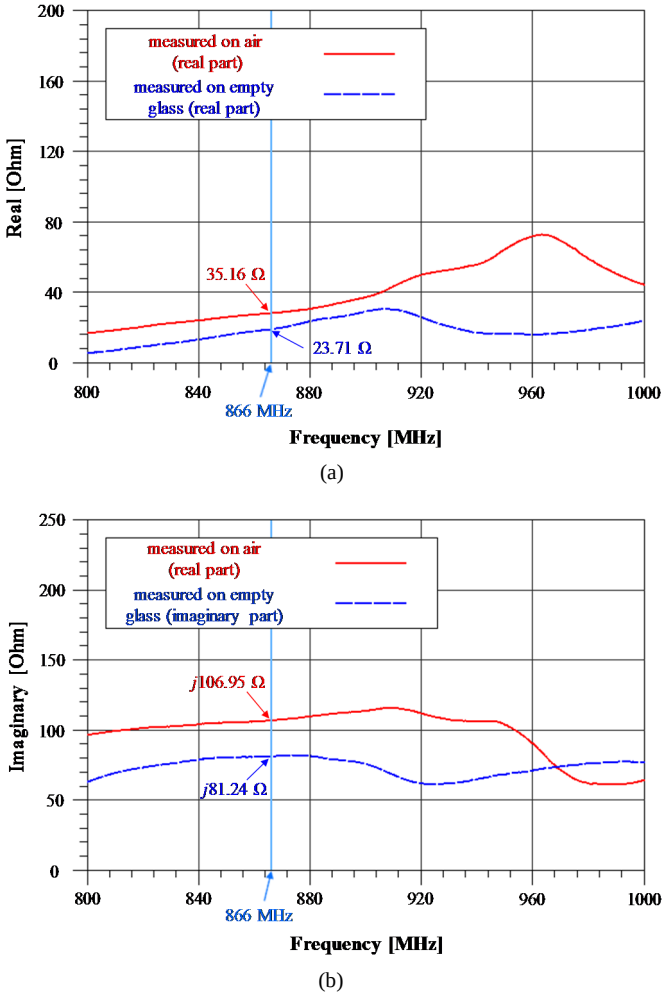

Figure 8 Measured impedance of the antenna of the RFID tag on air and mounted onto empty glass. (a) Real part. (b) Imaginary part. Results show the antenna has excellent conjugate match to the chip impedance that is 25.67 – *j*156.83 Ω (measured in Fig. 6).

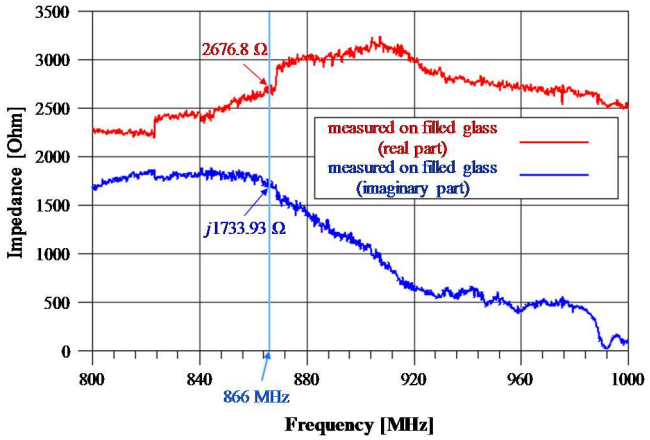

Figure 9 Measured impedance of the antenna of the RFID tag placed onto a water glass object filled with water.

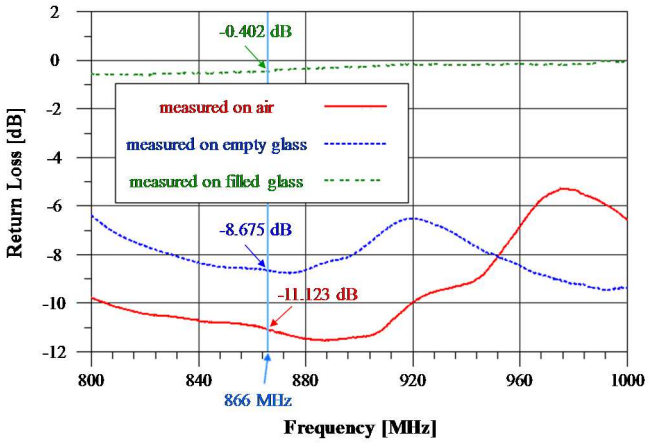

Figure 10 Measured return loss of the RFID tag antenna for three material surfaces, defined for input impedance of its RFID chip at threshold power.

REFERENCES

[1] J. Landt, "The history of RFID," *IEEE Potentials*, vol. 24, no. 4, pp. 8–11, Oct./Nov. 2005

[2] K. Finkenzeller, RFID Handbook: Fundamentals and Applications in Contactless Smart Cards and Identification. *John Wiley & Sons*, Second Edition, 2003

[3] K. V. S. Rao, P. V. Nikitin and S. Lam, "Antenna design for UHF RFID tags: a review and a practical application", *IEEE Transactions on Antennas and Propagation*, vol. 53, no. 12, pp. 3870-3876, Dec. 2005

[4] J. D. Griffin, G. D. Durgin, A. Haldi, and B. Kippelen, "RFID tag antenna performance on various materials using radio link budgets," *IEEE Antennas Wireless Propag. Lett*., vol. 5, no. 5, pp. 247–250, May 2006.

[5] P. V. Nikitin, K. V. S. Rao, S. Lam, V. Pillai, R. Martinez, and H. Heinrich, "Power reflection coefficient analysis for complex impedances in RFID tag design," *IEEE Trans. Microw. Theory Tech*., vol. 53, no. 9, pp. 2721–2725, Sep. 2005

[6] P. Nikitin, K. Rao, S. Lam, et al.: 'UHF RFID Tag Characterization: Overview and State-of-the-Art', *Antenna Measurement Techniques Association (AMTA)*, Seattle, WA, October 2012

[7] S. L. Kin, L. N. Mun, and P. H. Cole, "Investigation of RF cable effect on RFID tag antenna impedance measurement," *in Proc. IEEE Ant. & Prop. Sym.*, pp. 573-576, Jun. 2007

[8] A. S. Meier and W. P. Summers, "Measured impedance of vertical antennas over finite ground planes," *Proc. IRE*, vol. 37, no. 6, pp. 609–616, Jun. 1949.

[9] A. Ghiotto, T. Vuong, and K. Wu, 'Chip and Antenna Impedance Measurement for the Design of Passive UHF RFID Tag', *Proc. of the 40th European Microwawe Conf. (EuMC)*, Paris, France, Sep. 2010, pp.1086-1089

[10] K. D. Palmer and M. W. V. Rooyen, "Simple broadband measurements of balanced loads using a network analyzer," *IEEE Trans. Instrum. Meas*., vol. 55, no. 2, pp. 266–272, Feb. 2006

[11] X. Qing, K. G. Chean, and Z. N. Chen, "Impedance Characterization of RFID Tag Antennas and Application in Tag Co-Design", *IEEE Trans. Microwave Theory and Techniques*, vol. 57, no. 5, pp. 1268-1274, May 2009

[12] "De-embedding and Embedding S-parameter Networks Using a Vector Network Analyzer," *Agilent Application Note* 1364-1

[13] IE3D™ v.11.01 is a trademark of *Zeland Software Inc*., Fremont, CA, 2008.

[14] Sung-Lin Chen, Ken-Huang Lin, "Characterization of RFID Strap Using Single-Ended Probe", *IEEE Transactions on Instrumentation and Measurement*, vol.58, no.10, pp. 3619-3626, Oct. 2009

[15] Alien Technology Higgs 3 RFID chip specifications, available from: http://www.alientechnology.com/wp-content/uploads/Alien Technology-Higgs-3-ALC-360.pdf

[16] Nikitin, P., Rao, K., Martinez, R., *et al*.: 'Sensitivity and impedance measurements of UHF RFID chips', *IEEE Trans. Microw. Theory Tech.*, 2009, **57**, (5), pp. 1297–1302.

[17] Kronberger, R., Geissler, A., Friedmann, B.: 'New methods to determine the impedance of UHF RFID chips', IEEE Int. Conf. on RFID, Orlando, FL, USA, April 2010, pp. 260–265.

[18] Pozar, D.: 'Microwave Engineering' (John Wiley and Sons Inc., 2006, 3rd edn.)